Water Research 204 (2021) 117598

Contents lists available at ScienceDirect

Water Research

journal homepage: www.elsevier.com/locate/watres

Temperate climate energy-positive anaerobic secondary treatment of domestic wastewater at pilot-scale

Chungheon Shin [a,b,c,*], Sebastien H. Tilmans [a,b,c], Felipe Chen [c], Perry L. McCarty [a], Craig S. Criddle [a,b,c]

[a] Department of Civil and Environmental Engineering, Stanford University, 473 Via Ortega, Stanford, CA 94305, United States
[b] National Science Foundation Engineering Research Center for Re-Inventing the Nation's Urban Water Infrastructure (ReNUWIt), 473 Via Ortega, Stanford, CA 94305, United States
[c] Codiga Resource Recovery Center (CR2C), 692 Pampas Ln, Stanford, CA 94305, United States

ARTICLE INFO

Keywords:
Anaerobic membrane bioreactor (AnMBR)
Domestic wastewater treatment
COD removal
Energy balance
Operating expenses (OPEX)
Membrane fouling

ABSTRACT

Conventional aerobic secondary treatment of domestic wastewater is energy intensive. Here we report net energy positive operation of a pilot-scale anaerobic secondary treatment system in a temperate climate, with low levels of volatile solids for disposal (< 0.15 mgVSS/mg$COD_{removed}$) and hydraulic residence times as low as 5.3 h. This was accomplished with a second-generation staged anaerobic fluidized membrane bioreactor (SAF-MBR 2.0) consisting of a first-stage anaerobic fluidized bed reactor (AFBR) followed by a second-stage gas-sparged anaerobic membrane bioreactor (AnMBR). In stage 1, fluidized granular activated carbon (GAC) particles harbor methanogenic communities that convert soluble biodegradable COD into methane; in stage 2, submerged membranes produce system effluent (permeate) and retain particulate COD that can be hydrolyzed and/or recycled back to stage 1 for conversion to methane. An energy balance on SAF-MBR 2.0 (excluding energy from anaerobic digestion of primary suspended solids) indicated net energy positive operation (+ 0.11 kWh/m^3), with energy recovery from produced methane (0.39 kWh electricity/m^3 + 0.64 kWh heat/m^3) exceeding energy consumption due to GAC fluidization (0.07 kWh electricity/m^3) and gas sparging (0.20 kWh electricity/m^3 at an optimal flux of 12.2 L/m^2 h). Two factors dominated the operating expenses: energy requirements and recovery cleaning frequency; these factors were in turn affected by flux conditions, membrane fouling rate, and temperature. For optimization of expenses, the frequency of low-cost maintenance cleanings was adjusted to minimize recovery cleanings while maintaining optimal flux with low energy costs. An issue still to be resolved is the occurrence of ultrafine COD in membrane permeate that accounted for much of the total effluent COD.

1. Introduction

Great efforts are currently underway worldwide to reduce fossil fuel usage and to increase use of renewable sources of energy in response to the adverse impacts of fossil fuel usage on climate change. In the wastewater treatment sector, the major energy usage is the aeration required for operation of aerobic biological treatment systems. An alternative is anaerobic treatment, which can produce renewable energy in the form of methane gas while greatly reducing production of waste organic solids and their costly treatment and disposal (McCarty et al., 2011). Indeed, numerous full-scale anaerobic systems are used for treatment of concentrated waste streams such as domestic biosolids and industrial wastewaters, and even for treatment of low-strength streams, such as domestic wastewater, when ambient temperatures are sufficiently high or when a high efficiency of treatment is not required (Rittmann and McCarty, 2020).

In recent years, pilot-scale anaerobic membrane bioreactors (AnMBRs) have been evaluated for their potential to efficiently treat domestic wastewaters in temperate climates (Shin and Bae, 2018). A report by Evans et al. (2019) described comparative treatment results for two AnMBRs treating domestic wastewater. One is a common design, an Anaerobic Completely Stirred Tank Reactor followed by AnMBR (CSTR-AnMBR). This system relies upon dispersed growth plus use of gas-sparged ultrafiltration membranes for removal of biosolids from the system effluent (permeate) as well as to maintain high levels of biosolids in the treatment reactor. The second is a Staged Anaerobic Fluidized

* Corresponding author at: Department of Civil and Environmental Engineering, Stanford University, 473 Via Ortega, Stanford, CA 94305, United States.
E-mail address: lukeshin@stanford.edu (C. Shin).

https://doi.org/10.1016/j.watres.2021.117598
Received 5 May 2021; Received in revised form 30 July 2021; Accepted 21 August 2021
Available online 26 August 2021

Membrane Bioreactor (SAF-MBR) that includes an anaerobic fluidized-bed reactor (AFBR) in the first stage and ultrafiltration membranes in the second stage. In the AFBR, fluidized granular activated carbon (GAC) particles were used to harbor methanogenic communities that convert biodegradable COD into methane. In a first version of the SAF-MBR, membrane fouling control was achieved by allowing fluidized GAC particles to scour the membranes.

Both the CSTR-AnMBR and the SAF-MBR systems achieved COD removal efficiencies comparable to that of activated sludge. However, both had difficulties that deserve further research for improvement. The CSTR-AnMBR required a much longer detention time in order to hold sufficient microorganisms and meet the needed high solids retention time (SRT) for efficient anaerobic treatment. In addition, the high concentration of dispersed growth increased rates of membrane fouling and reduced membrane flux, both increased the membrane area required and the energy needed to control membrane fouling. The SAF-MBR operated efficiently at short detention times that were comparable to or better than those of typical aerobic treatment systems. But while GAC worked well for cleaning of membranes, that approach was too harsh and caused substantial membrane damage (Shin et al., 2016a; Evans et al., 2019).

The major conclusion from the Evans et al. (2019) report was, "To better capture the relative advantages of each system a hybrid AnMBR comprised of a GAC-fluidized bioreactor connected to a separate gas-sparged ultrafiltration membrane system is proposed. This will likely be more effective, efficient, robust, resilient, and cost-effective." We have now designed, fabricated, and operated the hybrid second generation system they proposed, referring to it as the SAF-MBR 2.0. To our knowledge this is the first report of net energy positive operation achieved by a pilot-scale AnMBR.

2. Methods and Materials

2.1. System configuration

A pilot-scale system, consisting of a microscreen for primary treatment followed by a SAF-MBR 2.0 for secondary treatment, was constructed at the Codiga Resource Recovery Center, (Stanford, CA). As illustrated in Fig. 1, primary treatment was achieved by pumping raw domestic wastewater through a grit removal system followed by a microscreen (MS-28, Hydro International, screen pore size = 300 μm). This screened effluent served as influent to SAF-MBR 2.0, which consisted of three reactors: AFBR 1 (1.0 m^3; 798 kg GAC), AFBR 2 (1.8 m^3; 1230 kg GAC), and a gas-sparged AnMBR (1.7 m^3). The AFBRs used fluidized GAC (Filtrasorb 300, Calgon Carbon) as a biocarrier. Originally, AFBR 2 was designed and operated as a particle-sparged AnMBR, but because of flow rate limitations, the particle-sparged AnMBR was converted to a second AFBR. AFBRs 1 and 2 were operated in parallel with external recirculation connecting them. To initiate operation, both reactors were seeded with active methanogenic biomass from an upflow anerobic sludge blanket (UASB) treating winery wastewater (E&J Gallo Winery, Fresno, CA). The pilot system then treated Stanford domestic wastewater for more than three years prior to this study. Constant upflow velocities were maintained at 43.8 m/h for AFBR 1 and at 27.1 m/h for AFBR 2.

A recirculation pump connected AFBR 2 to AFBR 1. Membrane-retained solids (MRS) from the AnMBR were recirculated throughout the system via a second recirculation loop connected to AFBR 1, enabling further hydrolysis of degradable suspended solids. Both recycled flows were twice the influent flow rate in order to maintain consistent MLSS concentrations in all three reactors. The solids retention time (SRT) for the system was controlled by continuously wasting MRS with a peristaltic pump (PU-77916-10, Masterflex) at a rate of 1% of influent flow.

The gas-sparged AnMBR was outfitted with three submersible membrane modules (ZeeWeed 500D, SUEZ) containing ultrafiltration membranes (nominal pore size 0.04 μm) and with two LEAPmbr diffusers (SUEZ) that provided biogas sparging of the membranes for fouling control. Only two of the three membrane modules were used to simulate high flux conditions (> 12 L/m^2 h) while maintaining the HRT (minimum of 5 h). Membrane fouling was controlled with four measures: (1) continuous ten-minute cycling with an 8 min permeate pumping period (pump on) followed by a 2 min relaxation period (pump off), (2) use of two LEAPmbr diffusers that provided continuous gas sparging of membrane modules at a specific gas demand per unit membrane area (SGD_m) of 0.21 Nm^3/m^2 h, (3) regular chemical maintenance cleaning (MC), and (4) chemical recovery cleaning (RC). MC consisted of two sequences of chemically enhanced backwashing (CEB). The first sequence used a 500 mg/L sodium hypochlorite solution; the second used a 2000 mg/L citric acid solution. Each MC sequence began with a 2 min initial CEB pulse followed by four 30 s CEB pulses at a flux of 20 L/m^2 h, each separated by a membrane relaxation period of 4.5

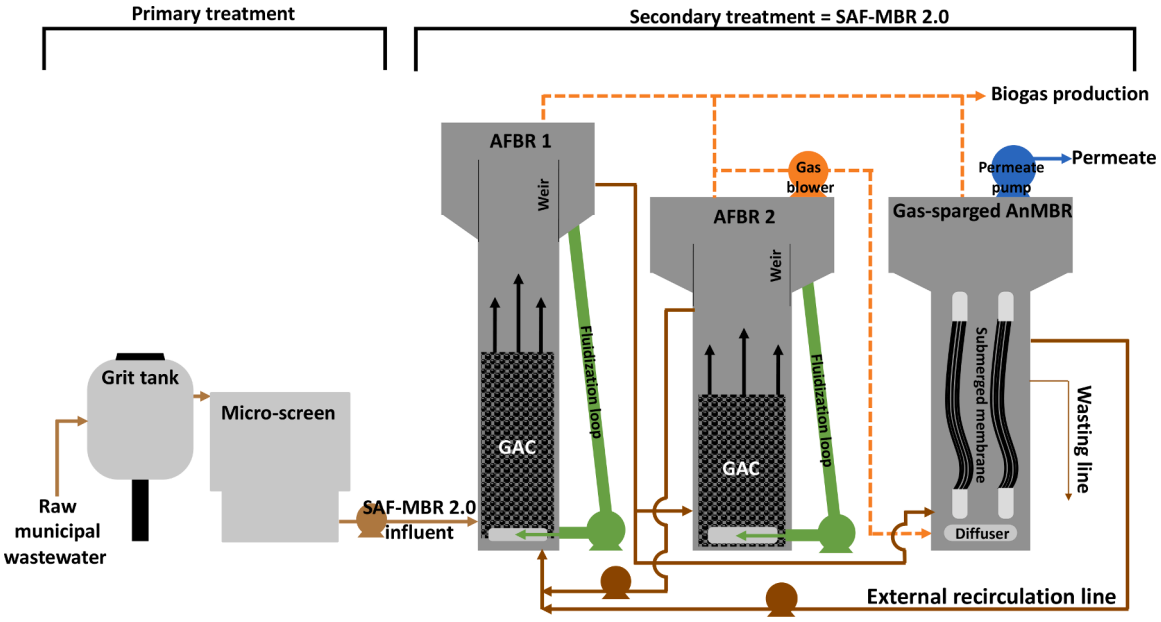

Fig. 1. A schematic diagram of the SAF-MBR 2.0 pilot scale system.

min. RC was conducted when the trans-membrane pressure (TMP) reached an upper limit set point (0.4 bar). During RC, the membrane tank was filled with an 1100 mg/L sodium hypochlorite solution, soaking the membranes in the solution for 24 h to eliminate organic foulant deposits. The tank was then flushed and filled with a citric acid solution (tank concentration of 2200 mg/L), and the membranes were soaked for another 24 h to remove inorganic foulants.

Table 1 contains a summary of conditions for each of the three different flux regimes used (after adjusting for the 20% relaxation period). The higher-flux third regime was subdivided into 2 sub-periods IIIa and IIIb when liquid temperatures differed significantly.

2.2. Sample collection and data analysis

Several system process parameters were monitored and logged continuously using a programmable logic controller (PLC) (CompactLogix, Allen Bradley). These parameters included fluidization loop pH and temperature (Signet 2724, GF), TMP (PX831, Omega Engineering Inc.), and influent and permeate flow rates (Signet 2551, GF). Biogas production was monitored continuously with mass flow meters (Alicat MW Series, Tucson, AZ), and biogas composition was monitored using a gas chromatograph equipped with a thermal conductivity detector (GC-TCD, Series 580, GOW-MAC, Bethlehem, PA) and an autosampler.

Raw wastewater and SAF-MBR 2.0 influent and effluent (permeate) were collected using composite samplers (5800 Refrigerated Sampler, Teledyne Isco). At each process stage, 500 mL samples were collected every 30 min, and then composited by mixing in a container prior to analysis. Grab samples were collected for MRS as its concentrations were less susceptible to diurnal fluctuations than constituent concentrations in raw wastewater. COD was monitored using a spectrophotometric method (EPA 410.4) using COD test tubes (Method 8000, Hach). Suspended solids (SS), alkalinity, and dissolved methane concentrations were measured using methods described in Shin et al. (2014). Acetate, propionate and sulfate concentrations in influent and permeate samples were analyzed by ion-chromatography (IC, Dionex™, Integrion™, HPIC™ System, Thermo Scientific; Column: Dionex IonPac AS11, Thermo Scientific).

Energy balances for the SAF-MBR 2.0 system were developed for each operational period. Energy inputs computed as per Shin and Bae (2018) included: (1) pumping energy for GAC fluidization in the AFBRs, (2) pumping energy for external recirculation among the three reactors, (3) pumping suction energy for permeate production, and (4) gas compression energy for membrane gas sparging. Energy outputs included: (1) computed energy from combustion of the recovered biogas methane (Shin and Bae, 2018), and (2) energy recovered from dissolved methane in the permeate (assumed recovery of dissolved CH_4 > 90%; operational energy requirement < 0.009 kWh/m^3, Crone et al. 2016). The efficiencies for gas blowers and combined heat and power (CHP) were modified with updated data. A CHP electrical conversion efficiency of 38% (Lang et al., 2017) and a blower energy efficiency of 65% (Lim et al., 2019) were assumed. More detailed information on energy calculations is provided in the Supporting Information.

Some influent biodegradable colloidal COD was found to be smaller than the pore size of the submerged membranes (40 nm). We refer to this fraction as ultrafine COD (UFCOD). Due to its small size, UFCOD can pass throught the membranes, limiting the efficacy of membrane-based size exclusion as a mechanism for its removal. To investigate this finding, we compared several characteristics of the influent UFCOD with those of the permeate. Influent UFCOD samples were obtained by filtering microscreen effluent (i.e., SAF-MBR 2.0 influent) through membrane filter paper (110,603, Whatman) with a pore size similar to that of the AnMBR membranes, then analyzed for COD. A dynamic light scattering (DLS) nanoparticle analyzer (Brookhaven Instrument Nanobrook Omni) was also used to measure nanometer-scale particle size distributions in the influent UFCOD. In addition, UFCOD hydrolysis rates were obtained using a set of parallel biochemical methane potential (BMP) batch tests in which BMP vials were seeded with SAF-MBR 2.0 GAC (18.75 g) along with one of several substrates (glucose, acetate, propionate, or SAF-MBR 2.0 influent UFCOD). These data were analyzed as part of a companion modeling study (Shin et al., 2021).

3. Results

3.1. COD removal

Table 2 contains summaries of COD concentrations and removal efficiencies for the overall system (microscreen + SAF-MBR 2.0) and for the SAF-MBR 2.0 alone during each operational period. The lowest overall COD removal was 87%. This value was observed during the period with the shortest HRT and lowest temperature (Period IIIb). SAF-MBR 2.0 COD removal was a function of HRT and temperature, varying from 84% at a 10 h HRT to 83% at a 7 h HRT in Period II, with further decreases in Period III at an HRT of 5.3 h: 79% in Period IIIa with > 20 °C temperature conditions, and 78% in Period IIIb with < 20 °C temperature conditions. These COD removal efficiencies were low compared with results from other pilot-scale AnMBR studies (> 87%, Shin and Bae 2018).

3.2. COD mass balance

Fig. 2 illustrates COD mass balances for periods II, IIIa and IIIb. The fraction of COD used by sulfate reducing bacteria was no greater than about 0.5 mg/L because of low influent sulfate (< 5 mgSO_4^{2-}/L). During Period II about 31% of the SAF-MBR 2.0 influent COD exited the system as permeate and as wasted MRS. During period IIIa with shorter HRT, this fraction increased to 37%, and then with lower temperature during period IIIb, it increased more to 42%. During Period IIIb, equipment malfunctions negatively affected methane gas measurements, resulting in an underestimate of gaseous methane.

3.3. Net positive energy

An energy balance was constructed for the SAF-MBR 2.0 pilot-system, comparing the energy for operation with the potential energy that could be obtained from the produced methane (Fig. 3). Data for Period IIIb was not used here because of the equipment caused gas measurement errors. Because the power required for system operation (kW) was constant, the required energy per cubic meter of flow (kWh/

Table 1
Operating conditions* of pilot-scale SAF-MBR 2.0 by operating period.

Period	Day	Influent Q (m^3/d)	Net flux (L/m^2-h)	HRT (h)	SRT (d)	OLR (kgCOD/m^3/d)	Temperature (°C)
I	1~77	10.8 (± 0.3)	6.5 (± 0.2)	10.0 (± 0.3)	45.1(± 0.0)	1.3 (± 0.2)	22.3 (± 1.9)
II	78~147	15.7 (± 1.4)	9.4 (± 0.9)	7.0 (± 0.7)	27.2 (± 0.0)	1.7 (± 0.4)	24.7 (± 1.1)
IIIa	148~203	20.5 (± 0.5)	12.3 (± 0.3)	5.3 (± 0.1)	21.6 (± 0.0)	2.3 (± 0.3)	22.5 (± 1.4)
IIIb	204~327	20.4 (± 0.7)	12.2 (± 0.4)	5.3 (± 0.2)	21.6 (± 0.0)	2.4 (± 0.5)	18.4 (± 1.5)

Q: flow rate.
OLR: organic loading rate.
*Mean values with standard deviation in (±).

Table 2
COD concentrations of raw wastewater, influent and SAF-MBR 2.0 permeate.

Period	HRT (h)	Temp. (°C)	COD concentration (mg/L)			COD removal (%)	
			Raw wastewater	SAF-MBR 2.0 influent	SAF-MBR 2.0 permeate	Overall removal	SAF-MBR 2.0 removal
I	10.0	22.3	720 (± 134)	538 (± 86)	84 (± 24)	90 (± 5)	84 (± 5)
		n	*8*	*56*	*56*	*8*	*56*
II	7.0	24.7	820 (± 222)	508 (± 96)	86 (± 24)	90 (± 7)	83 (± 5)
		n	*5*	*35*	*35*	*5*	*35*
IIIa	5.3	22.5	893 (± NA)	501 (± 59)	108 (± 26)	89 (+ NA)	79 (± 6)
		n	*1*	*25*	*25*	*1*	*25*
IIIb	5.3	18.4	834 (± 261)	529 (± 112)	115 (± 19)	87 (± 3)	78 (± 5)
		n	*6*	*26*	*26*	*6*	*26*

Overall COD removal efficiency = COD removal efficiency between raw wastewater and SAF-MBR 2.0 permeate.
n: number of data.
NA: not available.

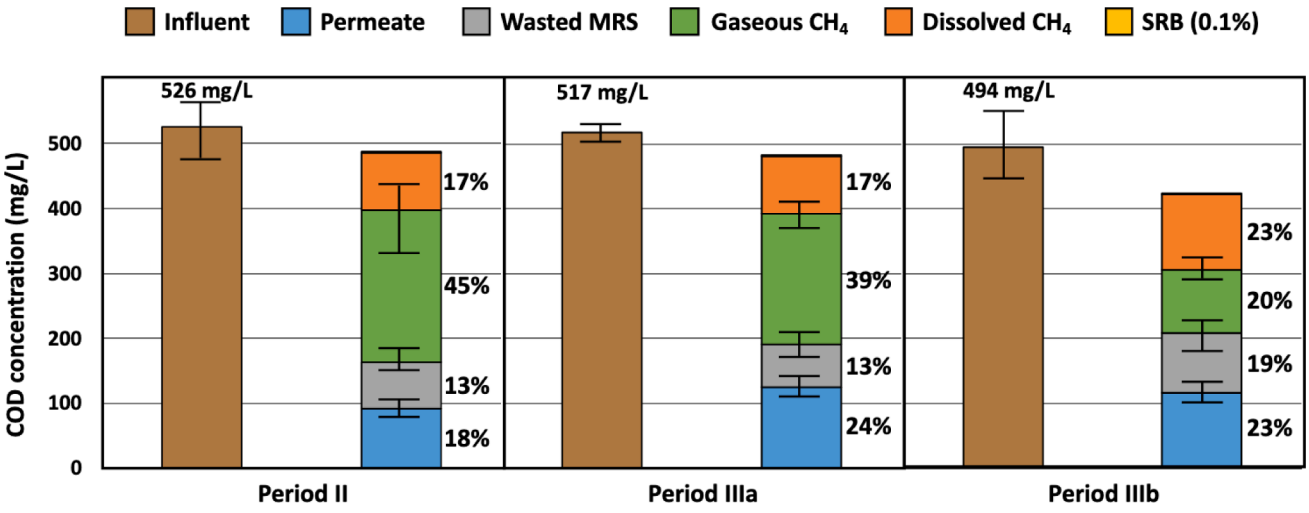

Fig. 2. COD mass balances over stable operational periods: Period II (days 80–109), Period IIIa (days 156–163), and Period IIIb (days 265–319).

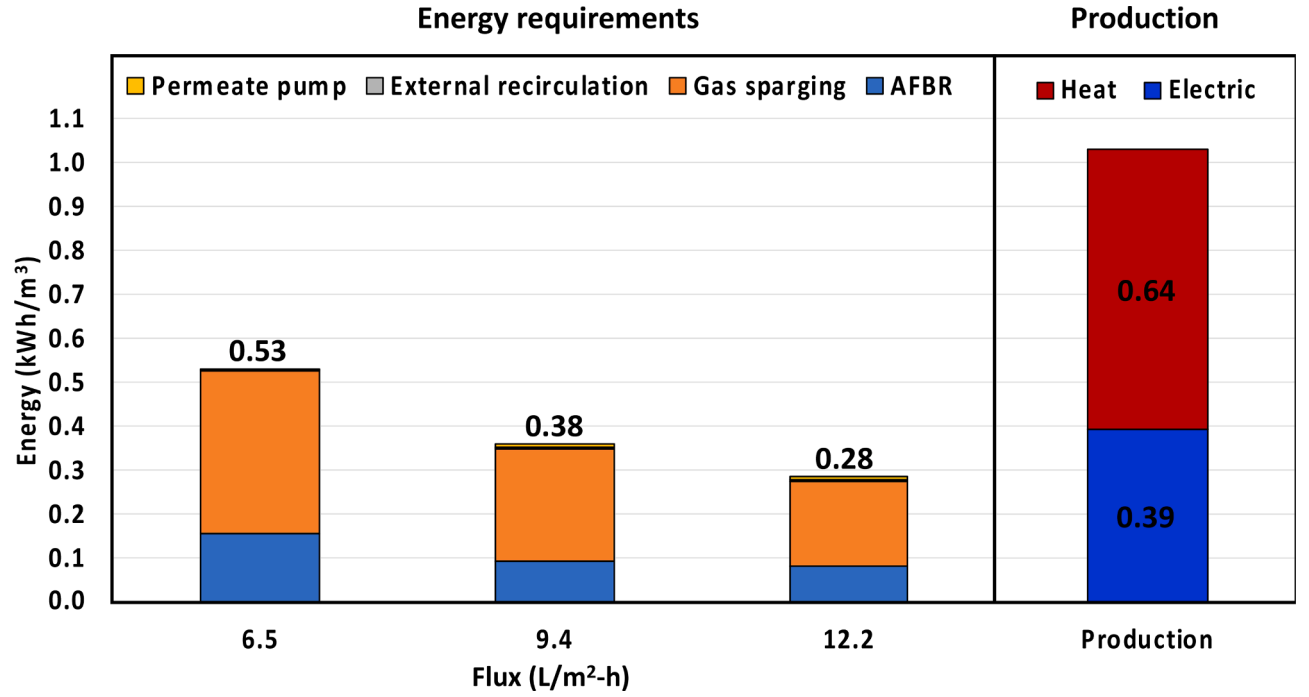

Fig. 3. Energy requirement (kWh/m^3) as a function of membrane flux (L/m^2-h) in periods I, II, and III (a and b), and the potential energy production (kWh/m^3) based upon observed methane production in periods II and IIIa when gas phase methane data was available without significant losses due to equipment malfunctions.

m^3) varied with flux as illustrated in Fig. 3.

Energy requirements for the SAF-MBR 2.0 ranged from 0.28 to 0.53 kWh/m^3. Gas sparging represented the largest fraction, comprising ~70% of total energy demand. As others have found (Crone et al., 2016), the energy required for recovery of dissolved methane using degassing membranes is less than ~0.01 kWh/m^3, much less than the energy required for gas sparging and fluidization.

Assuming 90% recovery of dissolved methane (Crone et al., 2016), mean energy production from all methane sources (gaseous and dissolved) for periods II and IIIa was 1.03 kWh/m^3. Typically, the energy conversion efficiency from combined heat and power (CHP) is 38% (Lang et al., 2017), so that the electrical energy produced would be 0.39 kWh/m^3, a value that exceeds the energy demand of 0.28 kWh/m^3 at a flux of 12.2 L/m^2-h by + 0.11 kWh/m^3.

The above analysis, however, does not include energy demands for preliminary and primary treatment, nor of that produced from anaerobic digestion of primary microscreened material. The additional energy demands (Longo et al., 2016), include influent pumps (< 0.04 kWh/m^3), grit removal (< 0.007, kWh/m^3), and microscreen filtration (0.01–0.02 kWh/m^3). These additional demands total 0.06–0.07 kWh/m^3 at the high end. On the positive side, additional electrical energy (0.12 kWh/m^3), about one-third of electrical energy produced from the secondary treatment (McCarty et al., 2011), would be generated from combustion of biogas produced by anaerobic digestion of the primary solids. This additional net energy production represents about 0.05–0.06 kWh/m^3, which when combined with the net increase of 0.11 kWh/m^3 from secondary treatment gives a net energy production of 0.16–0.17 kwh/m^3 (at the optimal net membrane flux of 12.2 L/m^2-h).

3.4. Removal of suspended solids and production of biosolids

Suspended solids in the influent, permeate and wasted MRS were monitored to quantify suspended solids removal and biosolids production for each operational period as summarized in TableS 3 and 4. The efficiency of suspended solids removal by membrane filtration was stable at 99 ± 1% and was unaffected by other operational conditions.

Table 4 contains a summary of mixed liquor suspended solids (MLSS) and mixed liquor volatile suspended solids (MLVSS) for operational periods (Periods II through IIIb) without SRT upsets. As expected, the VSS for disposal (active biomass plus unhydrolyzed VSS) per unit of COD removed increased from 0.08 to 0.13 mgVSS/mg$COD_{removed}$, likely due to less hydrolysis at lower SRT and lower temperatures. In a future full-scale implementation, wasted MRS containing appreciable COD due to operation at low SRT or at low temperature could be thickened and stabilized in an anaerobic digester, enabling additional energy recovery.

3.5. Membrane fouling and control measures

Fig. 4 illustrates changes in net flux and TMP together with temperature and chemical cleaning conditions, and Table 5 contains related values for the rate of change in membrane permeability (L/m^2-h/bar-day). These latter value (dK_{20}/dt) are corrected for temperature effects on viscosity by adjusting to the reference permeability at 20 °C (Shin et al., 2016b).

During Period 1, TMP was stable at a flux of 6.5 L/m^2 h without any significant increase. During Period II, TMP increased due to the higher flux (9.4 L/m^2 h). To mitigate fouling, the first recovery cleaning (RC) was carried out on day 136, and TMP recovered to levels comparable to the original TMP. During Period IIIa (12.3 L/m^2 h), membrane fouling rates increased rapidly and the permeability change rate dropped to -2.6 L/m^2 h/bar-day (Table 5). Accordingly, on day 164, the MC frequency was increased from once every two weeks to once every week. This increase effectively decreased the fouling rate to a value close to that of Period II. During Period IIIb, however, weekly membrane cleaning was insufficient to control the increased rate of fouling as temperatures dropped below 20 °C. Accordingly, a second RC was carried out on day 274 and the MC frequency was increased to twice weekly.

Increased chemical cleaning frequencies enabled flux values to reach 12 L/m^2 h. Evans et al. (2018) reported that a pilot-scale CSTR-AnMBR operating at MC and RC cycles similar to those used in this work and treating similar strength wastewater were subject to higher rates of membrane fouling at a flux of 10 L/m^2 h and required more intensive gas sparging. The lower membrane fouling rates in the SAF-MBR 2.0 were likely due to the much lower MRS in contact with the ultrafiltration membranes (Robles et al., 2013). The SAF-MBR 2.0, incorporating attached growth (GAC biocarrier within AFBR), maintained MLSS < 6000 mg/L at < 6 h HRT, with even lower values at 20 °C, while the CSTR-AnMBR had MLSS > 10,000 mg/L at > 10 h HRT (Evans et al., 2018).

3.6. High permeate COD traced to biodegradable UFCOD

Permeate COD during all operational periods was unexpectedly high, with concentrations ≥ 84 mg/L (Table 2), exceeding the United States COD secondary effluent standard of 60 mg/L (Lim et al., 2019). Several possible explanations for this high permeate COD were investigated, beginning with the possibility of membrane damage. Permeate grab samples from two sampling events were filtered through a laboratory-scale ultrafiltration module (prepared with 0.03 μm nominal pore size membranes, Samsung SDI), and analyzed in triplicate. There was no statistical difference between the permeate CODs measured before and after filtration. MRS filtered through a laboratory-scale ultrafiltration module had the same COD as pilot-scale permeate. Laboratory-scale ultrafiltration modules with fresh membranes did not enhance COD removal, illustrating that the submerged membranes were intact and functional.

Another possible explanation for the high permeate COD was the

Table 3
Pilot-scale SAF-MBR 2.0 total and volatile SS (TSS and VSS) concentrations in influent and permeate with SS removal efficiencies by operating periods.

	Period	I	II	IIIa	IIIb
	HRT (h)	10.0	7.0	5.3	5.3
	SRT (d)	45.1	27.2	21.6	21.6
	Temp. (°C)	22.3	24.7	22.5	18.4
Influent	TSS	112 (± 33)	111 (± 51)	102 (± 23)	139 (± 61)
	VSS	102 (± 34)	104 (± 49)	96 (± 21)	121 (± 52)
	n	31	49	21	38
Permeate	TSS	1 (± 1)	1 (± 1)	1 (± 1)	1 (± 1)
	VSS	1 (± 1)	1 (± 1)	1 (± 1)	1 (± 1)
	n	25	9	17	16
SS removal (%)		99 (± 1)	99 (± 1)	99 (± 1)	99 (± 1)

Table 4
MLSS and MLVSS concentrations and waste biosolids productions by operating periods.

Period*	II	IIIa	IIIb
HRT (h)	7.0	5.3	5.3
SRT (d)	27.2	21.6	21.6
Temp. (°C)	24.7	22.5	18.4
MLSS (mg/L)	3435 (± 646)	4304 (± 741)	5480 (± 939)
MLVSS (mg/L)	2987 (± 558)	3900 (± 657)	4618 (± 461)
N	39	19	22
Wasted VSS per COD removed** (mgVSS/mg$COD_{removed}$)	0.08 (± 0.03)	0.10 (± 0.02)	1.%2 (± 0.02)

* during Period 1, some unintended loss of solids occurred.

** $\frac{\text{Wasted VSS (mg/d)}}{\text{COD removed (mg/d)}} = \frac{\text{MLVSS (mg/L)} \times Q^w \text{ (L/d)}}{COD_{influent} \text{ (mg/L)} \times R\ (\%) \times Q^0 \text{ (L/d)}}$: Q^w = MRS wasting rate, Q^0 = influent flow rate, and R = SAF-MBR 2.0 COD removal efficiency.

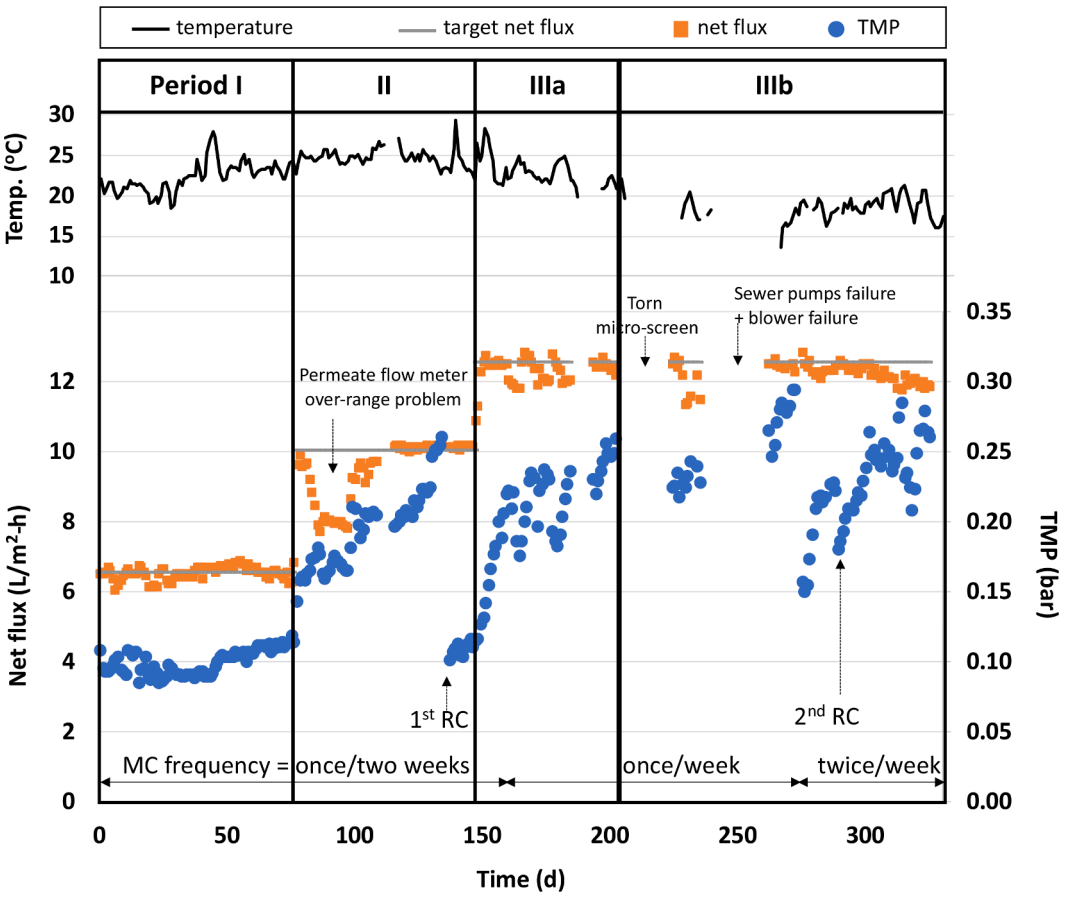

Fig. 4. Changes in operating temperature, net flux, and TMP during each operational Period.

Table 5
Permeability change rates (dK_{20}/dt) as a function of net flux, temperature and MC frequency.

Day	Net flux (L/m^2-h)	Temp. (°C)	MC frequency	dK_{20}/dt* (L/m^{2-}h/bar-day)
1 ~ 77	6.5	> 20	once/two weeks	-0.2
116 ~130	9.4	> 20	once/two weeks	-0.4
150 ~ 164	12.3	> 20	once/two weeks	-2.6
165 ~ 185	12.3	> 20	once/week	-0.2
263 ~ 273	12.2	< 20	once/week	-1.3
K	12.2	< 20	twice/week	-0.4

* dK_{20}/dt = normalized permeability change rate to 20 °C condition by normalizing flux to 20 °C (Shin et al., 2016b)

presence of influent refractory COD. Accordingly, BMP tests were used to assess the biodegradability of permeate COD (Shin et al., 2021). The measured and predicted volumes of methane (calculated from the permeate COD) were in good agreement, indicating that the permeate was fully biodegradable. Because acetate and propionate are major intermediates in methanogenesis, permeate samples were also analyzed by ion chromatography. Neither acetate nor propionate concentrations were above the detection limits for any operational period, even in permeate collected at low temperature.

To explore the possibility that permeate COD originated from influent colloidal organics, we measured particle size distributions for the influent UFCOD on a DLS nanoparticle analyzer, finding that the size of the influent UFCOD ranged between 18 and 33 nm (Fig. S1), smaller than the nominal ultrafiltration membrane pore size (40 nm). Further studies demonstrated that influent UFCOD is susceptible to hydrolysis. As it passes through ultrafiltration membranes, its hydrolysis would be governed by HRT, not SRT. In a companion modeling study (Shin et al., 2021), hydrolysis rates of influent UFCOD (k_{hyd}^{UF}) were independently determined. These values were used to predict the permeate COD at steady state for each operational period. The predictions matched measured values (Fig. 5), implying that unhydrolyzed influent UFCOD was likely the dominant contributor to permeate COD.

4. Discussion

4.1. Optimization of energy and chemical demands for membrane cleaning

This research underscores the trade-off between energy demand for system operation (largely due to fluidization and membrane sparging) verses chemical demands for membrane fouling control. Because power input to the pumps and blower was maintained constant, higher flux operation decreased energy demand but increased membrane fouling rates. Fouling rates can be controlled by implementation of an appropriate MC strategy Section 3.5). Fig. 6 illustrates estimated values for OPEX ($/m^3) over different periods of operation, including flux, energy requirements, MC frequency, RC interval, and membrane fouling rate (dK_{20}/dt). Energy costs were calculated from the energy demand (kWh/m^3), excluding energy from produced methane. Unit prices of energy and chemicals were $0.1/kWh, $279/m^3 for 14 % NaOCl solution, and $835/m^3 for 50% citric acid solution (Verrecht et al., 2010). Unit prices for MC and RC were $0.3 and $10.6 per cleaning event. The RC interval (T_{RC}) was determined from the membrane fouling rate (dK_{20}/dt,

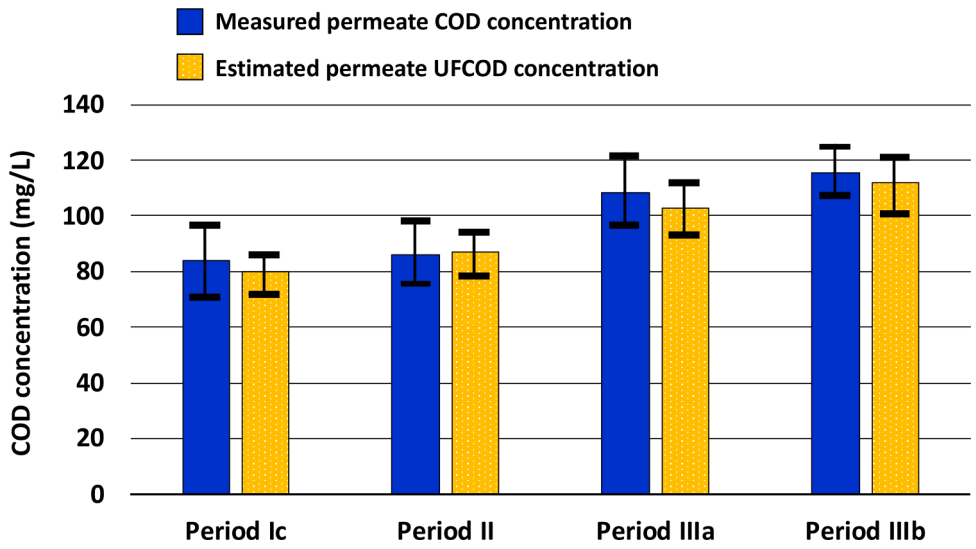

Fig. 5. Mean measured permeate COD and estimated permeate UFCOD by operational periods: Steady-state permeate UFCOD was estimated with an equation ($S_{UF} = \frac{S^0_{UF}}{1+k^{UF}_{hyd}\times HRT}$), temperature-corrected UFCOD hydrolysis rate constants (k^{UF}_{hyd}) based on (1.94 1/d at 20 °C, Shin et al., 2021) and monitored influent UFCOD concentration (S^0_{UF}, 140 ~ 170 mg/L) for each operational period.

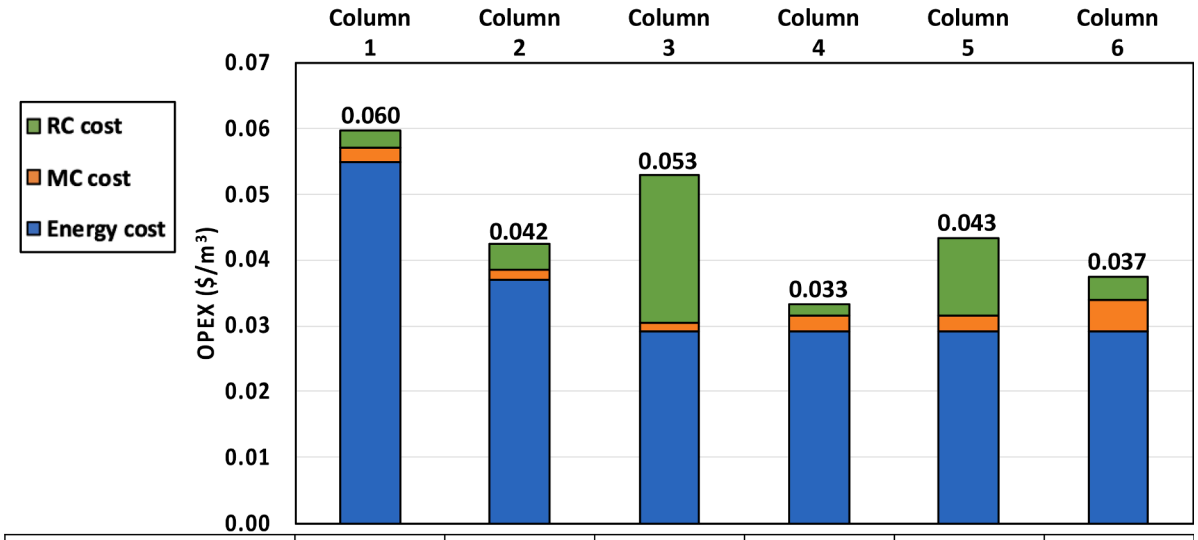

	Column 1	Column 2	Column 3	Column 4	Column 5	Column 6
Flux (L/m²/h)	6.5	9.4	12.3	12.3	12.2	12.3
Temperature (°C)	> 20	> 20	> 20	> 20	< 20	< 20
Fouling rate (dK_{20}/dt)	-0.2	-0.4	-2.6	-0.2	-1.3	-0.4
E requirement (kWh/m³)	0.56	0.34	0.27	0.27	0.27	0.27
MC frequency	Once /two weeks	Once /two weeks	Once /two weeks	Once /week	Once /week	Twice /week
RC interval (days)	362	180	23	292	45	151

Fig. 6. OPEX ($/m^3) variations depending on operating conditions (flux and temperature) and membrane fouling rate (dK_{20}/dt) (E: energy, MC: maintenance cleaning and RC: recovery cleaning).

L/m^2-h/bar-d), according to Eqs. (1) and ((2).

$$K_{20,\ min} = \frac{J_{20}}{TMP_{max}} \quad (1)$$

$$T_{RC} = \frac{K_{20,\ min} - K^0_{20}}{dK_{20}/dt} \quad (2)$$

where J_{20} is a normalized flux at 20 °C (Shin et al., 2016b) and TMP_{max} is the maximum TMP setpoint (0.4 bar). The $K_{20,\ min}$ is the minimum permeability for a given flux, which are 16.3, 23.5 and 31.3 L/m^2 h/bar at 6.5, 9.4 and 12.3 L/m^2 h flux conditions, respectively. K^0_{20} is the initial permeability (90 L/m^2 h/bar).

Energy costs (shaded blue fractions, Fig. 6) are the largest contributor to OPEX, greatly exceeding chemical costs for membrane cleaning,

and are driven by membrane flux. OPEX were highest for the lowest flux case of 6.5 L/m^2 h even though chemical cleaning requirements (green and orange fractions) were minimal. For operation at higher flux, proper selection of MC frequency became critical. At a flux of 9.4 L/m^2 h, OPEX dropped by 21% due to increased flux, but a further increase in flux to 12.3 L/m^2 h led to greatly increased fouling rates and larger OPEX because of shorter RC intervals (23 days as oppose to 180 days), which are more costly than MC cleanings. Increasing MC frequency from once every two weeks (column 3) to once per week (column 4) and RC interval from 23 days to 292 days minimized MC and RC costs for the 12.3 L/m^2 h case, enabling low OPEX at temperatures $>$ 20 °C (column 4). For temperatures $<$ 20 °C, operation under the same conditions (i.e., flux of 12.2 L/m^2 h with once weekly cleaning) led to increased rates of membrane fouling (column 5). This was addressed by increasing MC frequency to twice weekly and decreasing the RC interval to 151 days. The net effect of these changes was a decrease in OPEX. Taken together, these operational results underscore the importance of flux conditions and their impacts on energy demand. Also critical is the MC frequency and its impact on the interval required for more costly RC measures.

4.2. UFCOD effects and management

The high permeate COD observed in this study was unlike values obtained in previous pilot-scale studies of the SAF-MBR 1.0 (Shin et al., 2014), where effluent COD did not exceed 30 mg/L. This result may in part be explained by the more dilute influent COD of 270 mg/L in the earlier study (Shin et al., 2014) compared to the relatively high influent COD of ~520 mg/L in the present study. If we assume that doubling of the influent COD results in a doubling of permeate COD, then the expected permeate COD for the pilot-scale SAF-MBR 2.0 would be ~60 mg/L, but measured values were far greater (~120 mg/L). One possible explanation for the high permeate COD concentration is an unusually high UFCOD fraction (30%) in the influent, perhaps because the wastewater diverted from the Stanford Serra Street Sewer contained relatively fresh sewage and was subject to little hydrolysis prior to its collection. Other researchers have reported percentages of sub-micron colloid COD for domestic wastewaters ranging from 9 to 15% (Levine et al., 1991). In one study (Rickert and Hunter, 1971), the fraction of influent COD attributed to UFCOD colloidal organic matter was just 8% of the influent COD. Most pilot-scale AnMBR studies to date (Evans et al. 2018, summarized in Shin and Bae 2018) have likely had similar UFCOD fractions (i.e., close to ~10%). Due to size exclusion, the AnMBR can thus achieve $>$ 90% COD removal efficiency at any HRT depending upon membrane pore size. However, for cases with a high UFCOD fraction, like those of the present study, provisions need to be made for reduction of UFCOD in the influent or elsewhere, sufficient HRT for UFCOD hydrolysis, or modification of membranes. By increasing bioreactor volume, HRT could be increased while maintaining the same flux and membrane surface area, without any significant increase in energy demand for membrane fouling control. However, for influent UFCOD $>$ 150 mg/L, the HRT requirement could be $>$ 18 h to meet a secondary standard of 60 mg/L at 20 °C. This HRT is excessive for secondary treatment.

Not only is UFCOD a regulatory concern and a source of lost methane, it is also a critical membrane foulant. It can plug membrane pores, making it difficult to control clogging by gas sparging or membrane scouring – measures that are more effective for removal of cake layer foulants. The negative impacts of UFCOD on membrane permeate COD and fouling rates may differ for aerobic MBRs, where biological processes promote flocculation and coagulation (Rickert and Hunter, 1971), and hydrolysis rates may be more accelerated (Teo and Wong, 2014).

4.3. Needs for future study

SAF-MBR 2.0 achieved net energy positive operation while treating influent containing ~ 500 mgCOD/L. For more dilute influent, energy production would be less, but membrane fouling would also be less, potentially requiring less energy for gas sparging and/or lower chemical cost for MCs and RCs. The correlation between influent COD and membrane fouling rates needs further study, as does the role of UFCOD in membrane fouling, including strategies for its mitigation. A final issue that needs to be addressed is nutrient management and recovery (Shin and Bae, 2018).

5. Conclusions

A pilot-scale treatment train providing microscreened primary treatment and anaerobic secondary treatment with a SAF-MBR 2.0 system enabled $\geq$ 87% COD removal, 99% SS removal on a small footprint (HRT as low as 5.3 h), and stable operation under temperate conditions (18–25 °C). With the GAC biocarrier used, sufficient biomass was retained within the AFBR to enable efficient conversion of COD into methane. Moreover, because the active microorganisms were largely attached to activated carbon particles within the AFBR, the AnMBR compartment was operated efficiently with low levels of MRS ($<$ 6000 mg MLVSS/L), enabling operation at high flux ($>$ 12 L/m^2 h) and providing net positive energy operation. Energy costs constituted the largest fraction of operating expenses. Such costs could be reduced significantly by increasing the MC frequency. This cleaning strategy permitted much longer RC intervals. An unexpected discovery was the finding of significant biodegradable UFCOD, present as nanoparticles within the wastewater influent. This material was not removed by ultrafiltration, and adversely affected effluent COD. Control of such particles would be critical for compliance with regulatory standards.

Declaration of Competing Interest

The authors declare that they have no known competing financial interests or personal relationships that could have appeared to influence the work reported in this paper.

Acknowledgement

This research was supported by the Public Utilities Board (PUB), Singapore's National Water Agency (P17-12-03) and the National Science Foundation Engineering Research Center for Re-Inventing the Nation's Urban Water Infrastructure (ReNUWIt; EEC-1028968). A portion of this study was performed at the Stanford Nano Shared Facilities (SNSF)/Stanford Nanofabrication Facility (SNF), which is supported by the National Science Foundation under award ECCS-1542152. The membrane and LEAPmbr diffusion systems were provided by SUEZ. The authors thank Youngseck Hong and Jeff Cumin at SUEZ for technical advice in MBR installation and operation and the PUB team led by Ming Xiang Lim and Guihe Tao for project technical reviews. Dr. Shin's postdoctoral fellowship was funded with generous support from Olivia Chen. This research was conducted at the William and Cloy Codiga Resource Recovery Center at Stanford, a facility built with generous support from the Codiga family.

Supplementary materials

Supplementary material associated with this article can be found, in the online version, at doi:10.1016/j.watres.2021.117598.

References

Crone, B.C., Garland, J.L., Sorial, G.A., Vane, L.M., 2016. Significance of dissolved methane in effluents of anaerobically treated low strength wastewater and potential for recovery as an energy product: a review. Water Res. 104, 520–531.

Evans, P.J., Doody, A., Harclerode, M., Brower, A., Vila, P., McCarty, P.L., Parker, W., Parameswaran, P., Lim, K., Bae, J., Shin, C., Lee, P., Tan, A., Guy, K., Page, M., Maga, S., 2018, Anaerobic membrane bioreactor (AnMBR) for sustainable waste- water

treatment. In: Environmental Security Technology Certification Program Project (ESTCP Project ER-201434). https://www.serdp-estcp.org/Program-Areas/EnvironmentalRestoration/Wastewater-and-Drinking-Water/ER-201434.
Evans, P.J., Parameswaran, P., Lim, K., Bae, J., Shin, C., Ho, J., McCarty, P.L., 2019. A comparative pilot-scale evaluation of gas-sparged and granular activated carbon-fluidized anaerobic membrane bioreactors for domestic wastewater treatment. Bioresour. Technol. 288, 120949.
Lang, J., Schäffert, P., Böwing, R., Rivellini, S., Nota, F., Klausner, J., 2017. Development of a new generation of GE's Jenbacher type 6 gas engines. Heavy-Duty-, On-und Off-Highway-Motoren 2016. Springer Vieweg, Wiesbaden, pp. 19–36.
Levine, A.D., Tchobanoglous, G., Asano, T., 1991. Size distributions of particulate contaminants in wastewater and their impact on treatability. Water Res. 25 (8), 911–922.
Lim, K., Evans, P.J., Parameswaran, P., 2019. Long-term performance of a pilot-scale gas-sparged anaerobic membrane bioreactor under ambient temperatures for holistic wastewater treatment. Environ. Sci. Technol. 53 (13), 7347–7354.
Longo, S., d'Antoni, B.M., Bongards, M., Chaparro, A., Cronrath, A., Fatone, F., Lema, J. M., Mauricio-Iglesias, M., Soares, A., Hospido, A., 2016. Monitoring and diagnosis of energy consumption in wastewater treatment plants. A state of the art and proposals for improvement. Appl. Energy 179, 1251–1268.
McCarty, P.L., Bae, J., Kim, J., 2011. Domestic wastewater treatment as a net energy producer–can this be achieved? Environ. Sci. Technol. 45 (17), 7100–7106.
Rickert, D.A., Hunter, J.V., 1971. General nature of soluble and particulate organics in sewage and secondary effluent. Water Res. 5 (7), 421–436.
Rittmann, B.E., McCarty, P.L., 2020. Environmental Biotechnology: Principles And Applications, 2nd ed. McGraw-Hill Education.
Robles, A., Ruano, M.V., Ribes, J., Ferrer, J., 2013. Performance of industrial scale hollow-fibre membranes in a submerged anaerobic MBR (HF-SAnMBR) system at mesophilic and psychrophilic conditions. Sep. Purif. Technol. 104, 290–296.
Shin, C., McCarty, P.L., Kim, J., Bae, J., 2014. Pilot-scale temperate-climate treatment of domestic wastewater with a staged anaerobic fluidized membrane bioreactor (SAF-MBR). Bioresour. Technol. 159, 95–103.
Shin, C., Kim, K., McCarty, P.L., Kim, J., Bae, J., 2016a. Integrity of hollow-fiber membranes in a pilot-scale anaerobic fluidized membrane bioreactor (AFMBR) after two-years of operation. Sep. Purif. Technol. 162, 101–105.
Shin, C., Kim, K., McCarty, P.L., Kim, J., Bae, J., 2016b. Development and application of a procedure for evaluating the long-term integrity of membranes for the anaerobic fluidized membrane bioreactor (AFMBR). Water Science and Technology 74 (2), 457–465.
Shin, C., Bae, J., 2018. Current status of the pilot-scale anaerobic membrane bioreactor treatments of domestic wastewaters: a critical review. Bioresour. Technol. 247, 1038–1046.
Shin, C., Tilmans, S.H., Chen, F., Craig, C.S., 2021. Anaerobic membrane bioreactor model for design and prediction of domestic wastewater treatment process performance. Chem. Eng. J. 426, 131912.
Teo, C.W., Wong, P.C.Y., 2014. Enzyme augmentation of an anaerobic membrane bioreactor treating sewage containing organic particulates. Water Res. 48, 335–344.
Verrecht, B., Maere, T., Nopens, I., Brepols, C., Judd, S., 2010. The cost of a large-scale hollow fibre MBR. Water Res. 44 (18), 5274–5283.